Neutron cross sections for ^{3}He at epithermal energies

C. D. Keith,* Z. Chowdhuri,† D. R. Rich,‡ and W. M. Snow
Indiana University, Bloomington, Indiana 47408, USA

J. D. Bowman, S. L. Penttilä, and D. A. Smith§
Los Alamos National Laboratory, Los Alamos, New Mexico 87545, USA

M. B. Leuschner‖ and V. R. Pomeroy
University of New Hampshire, Durham, New Hampshire 03824, USA

G. L. Jones¶
National Institute of Standards and Technology, Gaithersburg, Maryland 20899, USA

E. I. Sharapov
Joint Institute for Nuclear Research, Dubna, Russia
(Received 30 October 2003; published 18 March 2004)

High accuracy, absolute measurements of the neutron total cross section for ^{3}He are reported for incident neutron energies 0.1–400 eV. The measurements were performed at the LANSCE short-pulse neutron spallation source. Using the previously determined cross section for neutron elastic scattering, 3.367 ± 0.019 b, we extract a new value for the energy dependence of the $^3\mathrm{He}(n,p)^3\mathrm{He}$ reaction cross section, $\sigma_{np} = (849.77 \pm 0.14 \pm 1.02)E^{-1/2} - (1.253 \pm 0.00 \pm^{+0.008}_{-0.049})$b, where the neutron energy is expressed in eV. The first uncertainty is statistical, the second systematic.

DOI: 10.1103/PhysRevC.69.034005 PACS number(s): 25.10.+s, 28.20.Cz, 28.20.Fc

I. INTRODUCTION

The scattering and absorption of neutrons by ^{3}He play key roles in many areas of nuclear physics. The ^{4}He compound nucleus formed during these processes is the lightest nuclear system known to possess a complex structure of excited states, and has long served as an important testing ground for few-nucleon calculations. For example, recent theoretical studies indicate that the α particle and its resonances may be particularly sensitive to the strength and character of three-nucleon ($3N$) forces [1,2]. The $^3\mathrm{He}(n,p)^3\mathrm{H}$ cross section appears as a sensitive parameter in most models of big-bang nucleosynthesis and forms the basis for a variety of low-energy neutron instruments, ranging from ionization chambers and scintillators to neutron spin polarizers and analyzers. This reaction has additionally served as a cross section standard for many years, due to its well-characterized energy dependence and the availability of isotopically pure ^{3}He.

It is not surprising then that a considerable amount of scattering and reaction data exists for the n-^{3}He interaction [3]. One area that is conspicuously lacking data is the epithermal energy region of about 1–500 eV. To our knowledge few experiments have been performed in this region.

Alfimenkov *et al.* published values for the total scattering cross section at energies 0.02–2 eV [4]. The measurements were calibrated against the ^{4}He scattering cross section and have been recently verified by a precise, spin-dependent scattering length measurement by Zimmer *et al.* [5]. The total cross section (scattering plus absorption) has been measured between 0.3 meV and 11 eV by Als-Nielsen and Dietrich [6], and in the range 0.025–250 eV by Alfimenkov *et al.* Unfortunately, the latter results were never made available except as a brief report in a not widely distributed publication [7]. Finally, Borzakov *et al.* [8] have published data for the $^3\mathrm{He}(n,p)^3\mathrm{H}$ cross section at energies as low as 250 eV. However, these measurements were made relative to the $^6\mathrm{Li}(n,a)^3\mathrm{H}$ reaction and ultimately normalized to the n-^{3}He *total* cross section data of Ref. [6], nearly two orders of magnitude lower in energy.

To address this situation, we have performed precise, absolute measurements of the neutron total cross section for ^{3}He at 4466 energies between 0.1 and 400 eV. Using the known scattering cross section for ^{3}He, we are able to perform a simple, polynomial fit to our data and obtain a cross section for the $^3\mathrm{He}(n,p)^3\mathrm{H}$ reaction with about 0.02% statistical and 0.1% systematic uncertainty. This reaction is strongly influenced by the presence of an unbound 0^+ state located between the p-^{3}H and n-^{3}He thresholds. Despite its discovery nearly 50 years ago [9], this state remains a topic of continued interest, and precise reaction data in the epith-

*Present address: Thomas Jefferson National Accelerator Facility, Newport News, VA 23606. Electronic address: ckeith@jlab.org
†Present address: National Institute of Standards and Technology, Gaithersburg, MD 20899.
‡Present address: Catholic University of America, Washington, DC 20064.
§Present address: Stanford Linear Accelerator, Stanford, CA 94309.
‖Present address: Indiana University Cyclotron Facility, Bloomington, IN 47408.
¶Present address: Hamilton College, Clinton, NY 13323.

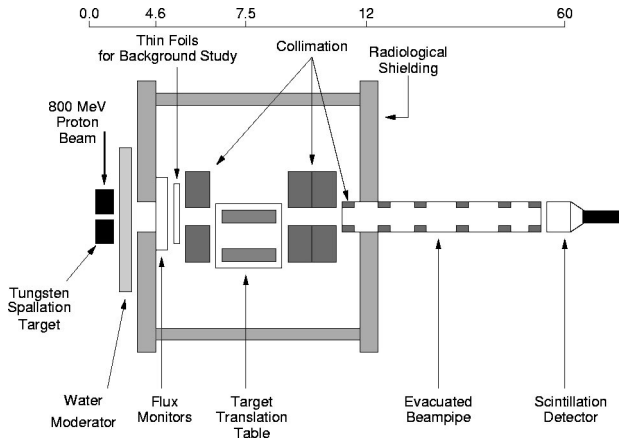

FIG. 1. Schematic layout of the total cross section experiment (not to scale). Approximate distances (in meters) from the neutron spallation target to the most important elements are indicated at the top.

ermal region are necessary to clarify its exact nature and the role that $3N$ forces may play in its structure [10].

Precise data for this reaction will also benefit neutron polarizers and analyzers based on polarized ^{3}He [11]. These instruments rely upon a strongly spin-dependent total cross section, which is almost completely determined by the $^3\mathrm{He}(n,p)^3\mathrm{H}$ reaction at low energies. In particular, the energy dependence of this reaction determines the energy dependence of the neutron polarization produced by a polarized ^{3}He spin filter, and it is useful to know the functional form of this dependence accurately.

The remainder of this paper is organized as follows. In Sec. II the experimental technique is detailed. The data analysis is described in Sec. III, and the results are presented and discussed in Sec. IV. A reduced, energy-averaged version of our data has been incorporated into a comprehensive R-matrix analysis of the $A=4$ system and the ^{3}He neutron scattering lengths [1].

II. EXPERIMENTAL TECHNIQUE

The total cross section was determined from target-in, target-out transmission measurements using the short-pulse neutron spallation source at the Los Alamos Neutron Science Center (LANSCE) [12]. A pulsed spallation source offers the unique opportunity to perform detailed studies of important systematic errors such as detector backgrounds. Such studies are prerequisite for any high accuracy measurement involving epithermal neutrons. This experiment utilized LANSCE Flight Path 2 which views the high-resolution water moderator of the spallation source. The time-of-flight (TOF) method was used to determine the neutron energy. A schematic diagram of the experimental layout is shown in Fig. 1.

The target consisted of 99.9999% pure ^{3}He gas contained within an aluminum cylinder 100.95 cm long, 8.0 cm in diameter, and with 0.30 cm thick endcaps. A statistically significant measurement of the total cross section could not be obtained using a single target thickness (areal density) because the cross section varies by two orders of magnitude over the energy range of our measurement. Instead, the experiment was performed with the target cylinder filled to four different gas pressures (see Table I). Deflection of the endcaps under these pressures was negligible. The sample cylinder was filled with ^{3}He while immersed in a stirred bath of water, usually at room temperature, to ensure temperature homogeneity. The temperature of the cell was measured at several locations using platinum resistors with calibration accuracies of 0.035 K. With this technique the average temperature of the cylinder could be determined with about 0.01% accuracy. A 6 mm diameter tube was used between the immersed cylinder and a room-temperature gas handling system to minimize the net transfer of heat to the cylinder from outside the bath. The cylinder was typically immersed for an hour or more to establish thermal equilibrium between the cylinder walls and ^{3}He gas, which could be observed by monitoring the gas pressure. This is considerably longer than the thermal time constant one expects for the system (a few minutes) based on the specific heats and thermal conductivities of aluminum and ^{3}He. The gas pressure was measured using a piezoresistive transducer with 0.01 kPa accuracy [13]. Corrections to the ideal gas law were applied using the second virial coefficient of ^{3}He [14], and were less than 0.5% in all cases.

The target cell was mounted on a computer-controlled translation table alongside an identical, evacuated cell. The two cells were alternately moved into and out of the neutron beam with 0.01 cm reproducibility every 2400 beam bursts (2 min). The ratio of dummy cell to target cell window thickness was 0.9951(3), as measured by neutron transmission with both cells evacuated.

A pair of ionization chambers was positioned just upstream of the target table to act as neutron flux monitors [15]. The first chamber was filled with ^{3}He gas, and the second

TABLE I. Summary of the neutron transmission experiments using four ^{3}He targets. A run consists of data acquired during 2400 beam bursts for both target-in and target-out conditions. The ^{3}He filling pressures and temperatures, P and T, are indicated foe each target, while nl is the product of the resultant number density and cell length.

Target	P (kPa)	T (K)	nl ($\times 10^{20}\mathrm{cm}^{-2}$)	t_{dwell} (μs)	E (eV)	Number of runs
1	31.59	273.64	8.44±0.01	0.5	0.11–3.0	93
2	99.95	292.47	25.00±0.02	1.0	0.38–8.3	126
3	300.17	292.49	75.16±0.05	2.0	6.8–72.2	188
4	672.10	291.87	167.82±0.12	5.0	15.3–392.7	383

with ^{4}He. The ^{4}He chamber responded only to γ rays produced at the spallation source, while the ^{3}He chamber responded to both γ rays and neutrons. The signals from both chambers were digitized by voltage-to-frequency converters and then subtracted to obtain a precise indication of the incident neutron flux.

The neutron beam was collimated both upstream and downstream of the target by a combination of lead and polyethylene, the latter loaded with either boron or lithium. The collimation, along with the small solid angle of the detector, eliminated the need for corrections due to nonforward angle scattering.

Neutrons transmitted through the target and collimators were detected 59.75 m away by a ^{3}He scintillation detector. This scintillator, which detected protons produced by the $^3\mathrm{He}(n,p)^3\mathrm{H}$ reaction ($Q=0.76$ MeV), was chosen due to its high efficiency for detecting low-energy neutrons, its fast time response ($\simeq$100 ns), and its insensitivity to γ rays. It consisted of an aluminum cylinder, 5 cm long and 5 cm in diameter, sealed at the upstream end by a 0.5 cm thick aluminum entrance window and at the downstream end by a 0.3 cm thick sapphire viewport. A single 5 cm diameter photomultiplier tube was coupled to the viewport. The cylinder was filled with 800 kPa of ^{3}He with 56 kPa xenon added for increased light output and improved pulse height resolution. The interior of the cylinder was coated with evaporated tetraphenylbutadiene which acted as a wavelength shifter for the vacuum ultraviolet scintillation light. A voltage feedback system was used to maintain a fixed pulse height spectrum, thereby stabilizing the gain of the photomultiplier tube. The noise induced in the photomultiplier tube by the voltage feedback system was measured and found to be less than the neutron counting statistics.

The data for each beam pulse were stored in a 9625 channel Ortec T914 multiscaler as a histogram of neutron count versus time of flight. The energy dependence of the time of flight was calibrated by inserting thin foils of ^{238}U, ^{191}Ir, and ^{193}Ir into the beam line. These nuclides possess a number of neutron resonances that appear as absorption peaks in the TOF spectra. The energies of seven of these resonances between 0.6 and 190 eV are known to 0.1% or better, and were used in a linear least-squares fit to determine L and t_o in the following TOF to energy relationship:

$$E_i = \frac{1}{2} m \left(\frac{L}{i(t_{\mathrm{dwell}} - t_o)} \right)^2 . \tag{1}$$

Here E_i is the neutron kinetic energy corresponding to the ith channel of the multiscaler, m is the neutron mass, L is the mean distance from the neutron spallation source to the scintillation detector, t_{dwell} is the width in microsecond assigned to each multiscaler channel, and t_o is a timing offset associated with the electronic start signal provided at the beginning of each beam pulse. An energy-dependent correction (maximum value 2 cm) was made to the extracted value of L to compensate for the fact that the lowest-energy neutrons were preferentially detected in the upstream end of the scintillator.

The precision of the TOF measurement depends both on the length of the flight path and the width of the initial proton pulse from the storage ring (250 ns). Further time broadening of the neutron pulse results from the moderation process and from the 15° angle between the flight path and the normal of the moderator surface. The resulting spread of the neutron pulse can be described as the sum of two convolutions between a Gaussian, characterized by a single full width at half maximum, and a pair of exponential tails, characterized by two decay constants [16]. Each of these response parameters depends upon the neutron energy, but at energies less than 500 eV they are 400–1500 times smaller than the actual neutron TOF. Though small, the effects of this time broadening are included in the software used to fit the seven calibration resonances. The precision to which an average neutron energy can be assigned for a given TOF bin is about 0.01%. The overall accuracy of our TOF calibration is therefore limited by the accuracy of the seven calibration resonances, about 0.1%.

The measurements are summarized in Table I.

III. DATA ACQUISITION AND ANALYSIS

The neutron total cross section was measured at $\approx$4500 energies between 0.1 eV and 400 eV. The data were acquired in the following manner. With the ^{3}He target cell in position, neutron counts from the scintillation detector were accumulated in the ith channel of the multiscaler for a period of time specified by t_{dwell}, after which the multiscaler advanced to the next channel. When the final multiscaler channel (or TOF bin) was reached, the multiscaler returned to the first channel and waited for the next beam burst, which was preceded by a start signal from the LANSCE spallation source. The same start signal was used to trigger a countdown scaler preset to a value of 2400. New counts in each TOF bin were accumulated on top of one another until the countdown scaler reads zero. At that time data acquisition was halted, the data from the multiscaler were written to disk, and the empty target cylinder was moved into place. A total of 790 of these "runs" were obtained for both the empty and ^{3}He targets. A typical TOF spectra is shown in Fig. 2.

The total cross section corresponding to a single TOF bin is then given by

$$\sigma_{\mathrm{tot}} = \frac{1}{nl} \ln \left(\frac{N_{\mathrm{out}}}{N_{\mathrm{in}}} \right), \tag{2}$$

where n and l are, respectively, the number density and length of the ^{3}He target, and N_{in} (N_{out}) is the observed number of neutron counts in the TOF bin after transmission through the ^{3}He (empty) target. In the off-line analysis the data N_{in} and N_{out} were normalized to the ionization chamber flux monitors and corrected for the difference in aluminum window thickness. Additional corrections were made for detector background, deadtime, and pulse pileup.

The detector background, which was primarily due to the multiple scattering of fast neutrons, was measured by inserting foils of Co, In, Ta, and Mn a few centimeters upstream of the target cells. These nuclides possess a number of resonances that were completely opaque to the neutron beam for

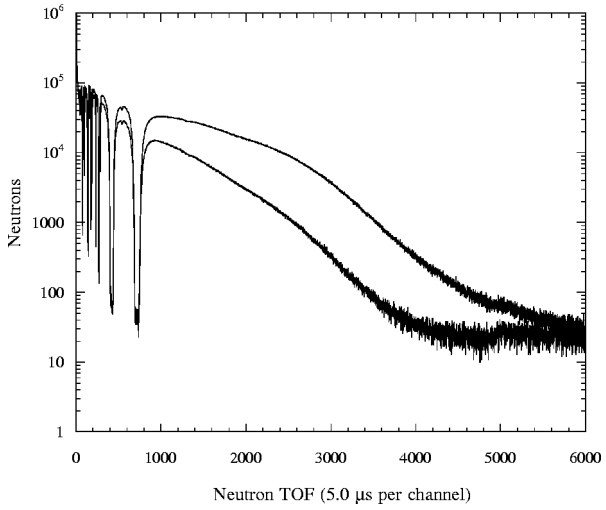

FIG. 2. A typical time-of-flight spectra corresponding to target number 4. The upper spectra correspond to the empty cylinder, the lower to the ^{3}He-filled cylinder. The large absorption peaks visible in both spectra result from foils of Co, In, Ta, and Mn which were inserted just upstream of the two target cylinders and used to determine the detector background.

the chosen foil thickness (the resonances are clearly visible in Fig. 2). A polynomial fit was applied to the bottoms of these opaque resonances on a run-by-run basis and subtracted from the TOF spectra. (These and other large resonances were excluded from the cross section analysis.) Additional measurements were performed with different foil thicknesses, which allowed us to extrapolate to a true background level. The background corrections to the total cross section were less than 0.1% except at the highest energies, where they reached 0.5%.

A comparison of the instantaneous detector rates (100 kHz for the empty target) and the 100 ns timing of the scintillation detector indicated a 1% order of magnitude for the detector deadtime. We expected the pileup to be of similar magnitude. To correct for these effects, we noted that, to first order, the observed detector rate Y in a given TOF bin differs from the true rate R in the following manner:

$$Y = R(1 - R\tau), \tag{3}$$

where τ is a parameter that includes the effects of both deadtime and pulse pileup. This relation holds true so long as $R\tau \ll 1$. From this we obtain the following relationship between the true cross section and the measured one [given by Eq. (2)]:

$$\sigma_{\text{true}} = \sigma_{\text{meas}} + \tau\frac{\Delta R}{nl}, \tag{4}$$

where ΔR is the observed difference between sample-in and sample-out detector rates.

We measured τ and its TOF dependence by repeating the sample-in, sample-out measurements using a carbon target. The neutron total cross section of carbon is known with a great accuracy and is energy independent over the entire range of our measurements [17]. The corrections to the ^{3}He cross section due to deadtime and pulse pileup amounted to less than 0.8% at the highest energies, and less than 0.1% at the lowest.

IV. EXPERIMENTAL RESULTS AND DISCUSSION

At the energies of interest here, the neutron total cross section for ^{3}He can be expressed as the sum of two parts: the scattering cross section σ_{nn} and σ_{np}, the cross section for the $^3\text{He}(n,p)^3\text{H}$ reaction. The cross section for radiative capture $\sigma_{n\gamma}$ is only a few microbarn [18], and can be neglected.

General expressions for the scattering and reaction cross sections can then be found in terms of the elastic scattering matrix,

$$S = e^{-2ik(a+ib)}. \tag{5}$$

By expanding S in terms of the neutron's center-of-mass wave number k, one finds that the cross sections can be written in the low-energy (i.e, long wavelength) limit as

$$\sigma_{nn} = \frac{\pi}{k^2}(1 - |S|^2) \approx 4\pi(a^2 + b^2) \tag{6}$$

and

$$\sigma_{np} = \frac{\pi}{k^2}|1 - S|^2 \approx 4\pi\left(\frac{b}{k} - 2b^2\right). \tag{7}$$

Here we see the familiar results that the scattering cross section for s-wave neutrons is independent of the neutron energy, and that the reaction cross section follows the well-known $1/v$ law. We also see in Eq. (7) that the first-order correction to the $1/v$ law is itself energy independent and *negative*.

Since the total cross section is the sum of σ_{nn} and σ_{np}, the transmission experiment reported here is unable to unambiguously separate the scattering cross section from the energy-independent contribution from σ_{np}. However, as first shown by Shapiro [19] an expression for the inelastic parameter b can be found in the limit $k \to 0$,

$$b = \frac{1}{4\pi}(\sigma_{np}k)_0, \tag{8}$$

where the subscript denotes evaluation at $k=0$. Inserting Eq. (8) into Eq. (7) and replacing k by the neutron's kinetic energy in the laboratory frame, $E = \hbar^2k^2m/\mu$, we arrive at the following expression for the total reaction cross section:

$$\sigma_{np} = A\left(\frac{1}{\sqrt{E}} - A\chi\frac{\mu^2}{\pi m\hbar^2}\right). \tag{9}$$

Here $A = (\sigma_{np}\sqrt{E})_0$, m is the neutron mass, and μ is the reduced mass of the $n + ^3$He system. The parameter

$$\chi = (2I + 1)\left[\frac{\chi_-^2}{I} + \frac{(1 - \chi_-)^2}{I + 1}\right] \tag{10}$$

is introduced to generalize the above relations to target spins $I \neq 0$. χ is a weighting factor for the $J = I - 1/2$ reaction channel, whose relative contribution to the cross section is χ_-.

TABLE II. Results of a least-squares fit to the total cross section using Eq. (11). The first uncertainty is statistical the second systematic. The number of time-of-flight bins used in each fit is indicated as is the reduced chi-squared ($\overline{\chi^2}$) for each fit.

Target	E_n (eV)	TOF bins	A (b eV$^{1/2}$)	$\overline{\chi^2}$
1	0.11–3.0	1652	$849.56 \pm 0.23 \pm 1.27$	0.95
2	0.38–8.3	1672	$850.35 \pm 0.22 \pm 0.98$	0.95
3	6.8–72.2	432	$850.31 \pm 0.35 \pm 0.97$	0.94
4	15.3–392.7	710	$848.59 \pm 0.31 \pm 0.92$	0.74
Combined	0.11–392.7	4466	$849.77 \pm 0.14 \pm 1.02$	0.94

Limits on χ_- have been set by two experiments. The transmission measurements of Passell and Schermer [20], performed with a polarized ^{3}He target and a polarized neutron beam, found $\chi_- = 1.010 \pm 0.032$. An even more stringent, though less direct constraint, $\chi_- = 0.998 \pm 0.01$, has been set by Borzakov *et al.* based on the departure of σ_{np} from the $1/v$ law [8]. Imposing the limit that $\chi_- \leqslant 1$, and taking the weighted average of the two values, we find $\chi = 3.986^{+0.014}_{-0.076}$.

We thus performed a linear least-squares fit of the form

$$\sigma_{\rm tot} = A\left(\frac{1}{\sqrt{E}} - A\frac{\chi\mu^2}{\pi m\hbar^2}\right) + \sigma_{nn} \tag{11}$$

to the 4466 data points using A as the only free parameter. The value for σ_{nn} was fixed at 3.367(19)b, the weighted average of the Alfimenkov [4] and Zimmer [5] cross sections, 3.37(2)b and 3.342(57)b, respectively [24]. A third preliminary value $\sigma_{nn} = 3.85(7)$ has been reported [21] but is not included in the average.

As a consistency check, we repeated the fit for each of the four ^{3}He target densities on an individual basis. The results are summarized in Table II. A complete tabulation of the 4466 cross section data points can be found in Ref. [22].

The combined result of all four targets yields a total reaction cross section (in barns) of

$$\sigma_{np} = (849.77 \pm 0.14 \pm 1.02)E^{-1/2} - (1.253 \pm 0.00 \pm^{+0.008}_{-0.049}), \tag{12}$$

where the neutron energy is expressed in eV. The first uncertainty is statistical, the second systematic. This value of σ_{np} is in agreement with the value previously extracted from the total cross section data of Als-Nielsen and Dietrich below 11 eV [6]:

$$\sigma_{np} = (847.5 \pm 1.5)E^{-1/2} \tag{13}$$

and extrapolates to a value of $5341.21 \pm 0.88 \pm 6.41$ b at the thermal energy of 0.0253 eV.

A reduced (energy-averaged) set of the total cross section data and our fit to the data are plotted in Fig. 3. For clarity, the data are plotted as $\sigma_{\rm tot}E^{1/2}$ versus neutron energy. Our extracted polynomial for σ_{np} is also shown as are the results from previous measurements.

If we repeat the least-squares fit of our data including σ_{nn} as a free parameter, we obtain $\sigma_{nn} = 3.1 \pm 0.05 \pm 1.1$ b. Thus we cannot improve upon the accuracy of this cross section.

V. CONCLUSIONS

We have reported an absolute measurement of the neutron total cross section for ^{3}He in the energy range 0.1–400 eV. Exploiting the known value for the scattering cross section, we have extracted the cross section for the ^{3}He$(n,p)^3$H reaction σ_{np} with about 0.1% accuracy, and we find good agreement with previous measurements of this quantity.

Our extraction of σ_{np} also relied upon prior knowledge of the spin dependence of this cross section, characterized here by χ_-, which is presently known with a precision of about 2%. While a significantly improved measurement of χ_- would have minimal impact on σ_{np}, it would improve the present uncertainties in the n-^{3}He scattering lengths. For example, the most precise measurement yet reported for the incoherent scattering length b_i' [5] is largely limited by uncertainty in χ_-. A threefold improvement in the latter would

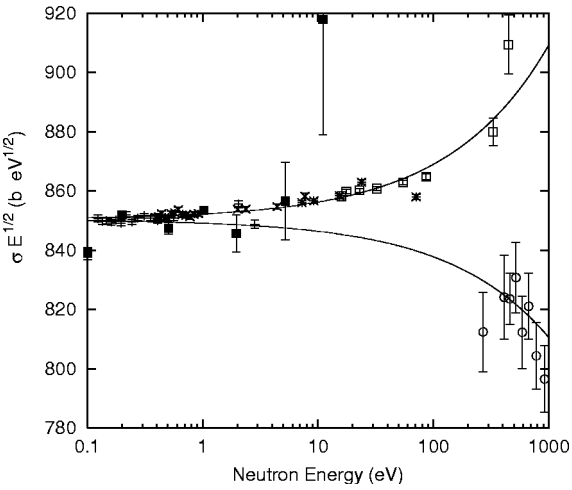

FIG. 3. Measured neutron total cross section data (energy averaged) plotted as $\sigma_{\rm tot}\sqrt{E}$ vs neutron energy: target 1 (+), target 2 ($\times$), target 3 (*), target 4 ($\square$). The error bars represent statistical uncertainties only. The upper curve is a least-squares fit to $\sigma_{\rm tot}$ using Eq. (11). The lower curve is the ^{3}He$(n,p)^3$H reaction cross section extracted from our data [Eq. (12)]. Also shown are fringe points from the $\sigma_{\rm tot}$ measurement of Ref. [6] (solid squares), and σ_{np} data from Ref. [8] (circles). The downward curve of σ_{np} is due to a negative contribution to the reaction cross section [Eq. (7)]; a strict $1/v$ dependence would be seen as a flat line in this graph. The upward curve of $\sigma_{\rm tot}$ reveals the presence of the scattering cross section.

lower the uncertainty in b_i' by more than a factor of 2. However, a direct, absolute determination of χ_- requires both polarized target and beam, and is therefore subject to additional systematic errors.

Finally, four-body calculations of the ^{4}He system using realistic *NN* and 3*N* potentials have now reached a high level of sophistication, and their interpretation is primarily limited by the quality of experimental data. High precision data at all energies are now necessary as a basis for new theoretical understanding.

Note added in proof. The authors have recently been informed of a new value for σ_{nn}, 3.279 ± 0.008, obtained from a measurement of the ^{3}He coherent scattering length using neutron interferometry [25]. Combined with the two previous measurements of σ_{nn} cited in this article, a new average value of 3.292 ± 0.0074 is obtained. The resulting change in the reaction cross section extracted from our total cross section data is neglible, $\sigma_{np} = 849.92E^{-1/2} - 1.253$ *b*.

ACKNOWLEDGMENTS

This work was benefited from the Los Alamos Neutron Science Center at the Los Alamos National Laboratory, a facility funded by the U.S. Department of Energy and operated by the University of California under Contract No. W-7405-ENG-36. This research was supported in part by the U.S. Department of Energy, Office of High Energy and Nuclear Physics, under Grant No. DE-FG02-96-ER45587 and by NSF CAREER Grant No. NSF-PHY-9501312.

[1] H. M. Hofmann and G. M. Hale, Phys. Rev. C **68**, 021002 (2003).
[2] H. M. Hofmann and G. M. Hale, in *High Performance Computing in Science and Engineering, Munich 2002*, edited by S. Wagner, W. Hanke, A. Bode, and F. Durst (Springer-Verlag, Berlin, 2003), p. 389.
[3] D. R. Tilley, H. R. Weller, and G. M. Hale, Nucl. Phys. **A541**, 1 (1992), this compilation paper contains a complete reference guide to experimental and theoretical work on $A=4$ nuclei since 1973.
[4] V. P. Alfimenkov *et al.*, Sov. J. Nucl. Phys. **25**, 607 (1977).
[5] O. Zimmer *et al.*, Eur. Phys. J. A **1**, 1 (2002).
[6] J. Als-Niesen and O. Dietrich, Phys. Rev. **133**, B925 (1964).
[7] V. P. Alfimenkov *et al.*, in *Translation of Selected Papers Published in Nuclear Constants* (International Nuclear Data Committee, Vienna, 1982), Vol. 1, pp. 27–30.
[8] S. B. Borzakov *et al.*, Sov. J. Nucl. Phys. **35**, 307 (1982).
[9] R. M. Frank and J. L. Gammel, Phys. Rev. **99**, 1405 (1955).
[10] H. M. Hofmann (private communication).
[11] D. R. Rich *et al.*, Nucl. Instrum. Methods Phys. Res. A **481**, 431 (2002), a more detailed discussion of the systematic uncertainties encountered in the present experiment may be found in this paper, which describes a polarization measurement utilizing the same beam line, electronics, and data acquisition techniques.
[12] J. D. Bowman *et al.*, Nucl. Instrum. Methods Phys. Res. A **297**, 183 (1990).
[13] Mensor Digital Pressure Gauge Series 2101, Mensor Corp., San Marcos, TX 78666. The accuracy of this gauge was confirmed by NIST-traceable standards both before and after the experiment.
[14] J. J. Hurly and M. R. Moldover, J. Res. Natl. Inst. Stand. Technol. **105**, 667 (2000).
[15] J. J. Szymanski *et al.*, Nucl. Instrum. Methods Phys. Res. A **340**, 564 (1994).
[16] Yi-Fen Yen *et al.*, Nucl. Instrum. Methods Phys. Res. A **447**, 476 (2000).
[17] J. Schmiedmayer, H. Rauch, and P. Riehs, Phys. Rev. Lett. **61**, 1065 (1988).
[18] F. L. H. Wolfs *et al.*, Phys. Rev. Lett. **63**, 2721 (1989).
[19] F. L. Shapiro, Sov. J. Nucl. Phys. **7**, 1132 (1958).
[20] L. Passell and R. I. Schermer, Phys. Rev. **150**, 146 (1966).
[21] K. Guckelsberger, W. Nistler, R. Scherm, and M. Weyrauch, Physica B **276–278**, 975 (2000).
[22] D. R. Rich, Ph.D thesis, Indiana University, 1999.
[23] H. Kaiser *et al.*, Z. Phys. A **291**, 231 (1979).
[24] It should be noted that Alfimenkov *et al.* reported a scattering cross section of 3.17 b in Ref. [4]. This value was subsequently rescaled following a more precise measurement of the ^{4}He scattering length [23].
[25] P. R. Huffman *et al.*, Phys. Rev. C (submitted).